Precision Nucleon-Nucleon Potential at Fifth Order in the Chiral Expansion

E. Epelbaum,[1] H. Krebs,[1] and U.-G. Meißner[2,3,4]

[1]*Institut für Theoretische Physik II, Ruhr-Universität Bochum, D-44780 Bochum, Germany*

[2]*Helmholtz-Institut für Strahlen- und Kernphysik and Bethe Center for Theoretical Physics, Universität Bonn, D-53115 Bonn, Germany*

[3]*Institut für Kernphysik, Institute for Advanced Simulation, and Jülich Center for Hadron Physics, Forschungszentrum Jülich, D-52425 Jülich, Germany*

[4]*JARA–High Performance Computing, Forschungszentrum Jülich, D-52425 Jülich, Germany*

(Received 15 December 2014; revised manuscript received 15 May 2015; published 17 September 2015)

We present a nucleon-nucleon potential at fifth order in chiral effective field theory. We find a substantial improvement in the description of nucleon-nucleon phase shifts as compared to the fourth-order results utilizing a coordinate-space regularization. This provides clear evidence of the corresponding two-pion exchange contributions with all low-energy constants being determined from pion-nucleon scattering. The fifth-order corrections to nucleon-nucleon observables appear to be of a natural size, which confirms the good convergence of the chiral expansion for nuclear forces. Furthermore, the obtained results provide strong support for the novel way of quantifying the theoretical uncertainty due to the truncation of the chiral expansion proposed by the authors. Our work opens up new perspectives for precision *ab initio* calculations in few- and many-nucleon systems and is especially relevant for ongoing efforts towards a quantitative understanding of the structure of the three-nucleon force in the framework of chiral effective field theory.

DOI: 10.1103/PhysRevLett.115.122301 PACS numbers: 13.75.Cs, 21.30.-x

Chiral effective field theory (EFT) provides a solid foundation for analyzing low-energy hadronic observables in harmony with the symmetries of QCD, the underlying theory of the strong interactions. It allows one to derive nuclear forces and currents in a systematically improvable way order by order in the chiral expansion, based on a perturbative expansion in powers of $Q \in (p/\Lambda_b, M_\pi/\Lambda_b)$, where p refers to the magnitude of three momenta of the external particles, M_π is the pion mass, and Λ_b is the breakdown scale of chiral EFT [1]. Being combined with modern few- and many-body methods, the resulting framework based on solving the nuclear A-body Schrödinger equation with interactions between nucleons tied to QCD via its symmetries represents nowadays a commonly accepted approach to *ab initio* studies of nuclear structure and reactions; see Refs. [2,3] for review articles.

Chiral power counting suggests that nuclear forces are dominated by pairwise interactions between the nucleons [1], a feature that has been conjectured for a long time but could only be explained with the advent of chiral EFT. Many-body forces are suppressed by powers of the expansion parameter Q. Specifically, the chiral expansion of nucleon-nucleon (NN), three-nucleon (3NF), and four-nucleon (4NF) forces starts at the orders Q^0 (LO), Q^3 ($\mathrm{N^2LO}$), and Q^4 ($\mathrm{N^3LO}$), respectively, while next-to-leading (NLO) corrections involve two-body operators only. While accurate NN potentials at $\mathrm{N^3LO}$ have been available for about a decade [4,5], the 3NF still represents one of the major challenges in the physics of nuclei and nuclear matter [6]. In particular, numerically exact calculations in the three-nucleon (3N) continuum, the most natural place to test the 3NF, have revealed that the spin structure of the 3NF is not properly reproduced by the available models [7]. Specifically, one observes clear discrepancies between theory and experimental data for various spin observables in nucleon-deuteron (Nd) scattering starting at $E_N \sim 50$ MeV, which tend to increase with energy. In addition, there are a few discrepancies at low energies such as, e.g., the so-called A_y puzzle; see Ref. [7] for more details.

In the framework of chiral EFT, the impact of the leading 3NF at $\mathrm{N^2LO}$ on three- and four-nucleon scattering, nuclear structure, and reactions, as well as nuclear matter, has been extensively studied using different many-body techniques. In particular, the $\mathrm{N^2LO}$ 3NF was found to reduce the discrepancy for A_y in proton-^{3}He elastic scattering [8] and to play a crucial role in understanding neutron-rich systems [9] and the properties of neutron and nuclear matter; see [6] and references therein. Lattice simulations of light nuclei within the framework of chiral EFT also confirm the important role of the $\mathrm{N^2LO}$ 3NF [10–12]. On the other hand, the A_y puzzle in elastic Nd scattering is not resolved at $\mathrm{N^2LO}$ [8], and the existing discrepancies for spin observables in the 3N continuum at medium and higher energies are beyond the expected theoretical accuracy at this order. It is, therefore, necessary to study corrections beyond the leading 3NF. The $\mathrm{N^3LO}$ contributions to the 3NF have been worked out recently and appear to be parameter free [13,14]. It was found, however, that the chiral expansion of the long- and intermediate-range parts of the 3NF is not converged at this order due to large fifth-order ($\mathrm{N^4LO}$) corrections associated with intermediate

$\Delta(1232)$ excitations [15–17]. A resolution of the long-standing discrepancies in the 3N continuum will, therefore, likely require the knowledge of the nuclear Hamiltonian at N^{4}LO [18].

In this Letter, we make an important step along this line and present the NN potential at fifth order in the chiral expansion based on the improved regularization framework introduced in Ref. [19]. In addition to constructing a new state-of-the-art chiral NN potential that leads to an excellent description of the data and is expected to provide a solid basis for future few- and many-body calculations, our study represents a highly nontrivial test of the convergence of the chiral expansion and of the new approach for estimating the theoretical uncertainty, a necessary ingredient of any EFT calculation [20].

We first discuss the isospin-conserving part of the potential. As described in detail in Ref. [19], the NN potential at N^{3}LO involves contributions from up to three-pion exchange and contact interactions acting in S, P, and D waves and the mixing angles ϵ_1 and ϵ_2. When expressed in terms of physical values of the pion masses and pion-nucleon (πN) coupling constant, the expression for the one-pion exchange potential (OPEP) remains unchanged at N^{4}LO. On the other hand, the static two-pion exchange potential (TPEP) receives corrections at fifth order that are visualized in Fig. 1. The corresponding diagrams up to the two-loop level have been calculated recently using the Cutkosky rules [21]. We have independently calculated these contributions and have verified the expressions presented in that work. Next, one also needs to account for the Goldberger-Treiman discrepancy and the leading relativistic corrections to the order Q^3 TPEP. Notice that the latter were already taken into account in Ref. [19]. Furthermore, in addition to the TPEP, one encounters subleading three-pion exchange diagrams at N^{4}LO. Similar to Refs. [4,5,19], we do not include the three-pion exchange potential explicitly, assuming that its effects can be well reproduced by contact interactions. We have verified the validity of this assumption for the intermediate value of the regulator [22]. A remarkable feature of the N^{4}LO NN potential is the absence of new isospin-conserving contact interactions. This can be traced back to parity conservation and to the fact that the N^{4}LO corresponds to an odd power of the expansion parameter, namely, Q^5. This feature allows one to unambiguously probe the impact of the fifth-order TPEP in NN scattering.

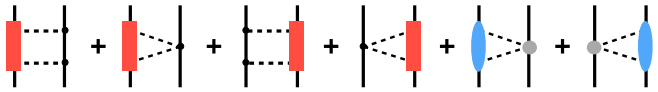

FIG. 1 (color online). Fifth-order contributions to the TPEP. Solid lines and dashed lines refer to nucleons and pions, respectively. Solid dots denote vertices from the lowest-order πN effective Lagrangian. Filled (red) rectangles, (blue) ovals, and gray circles denote the order Q^4, order Q^3, and order Q^2 contributions to πN scattering, respectively.

Our treatment of isospin-breaking (IB) corrections is limited to the one employed in the Nijmegen partial wave analysis (NPWA) [23], which is used as input in our calculations; see Ref. [19] for more details. The only new IB contribution we include compared to the N^{3}LO analysis of Ref. [19] is the momentum-dependent contact interaction in the $^1S_0$ channel, which results in $C_{1S0}^{\rm pp} \neq C_{1S0}^{\rm np}$ using the notation of that work.

It remains to specify the values of the various parameters entering the potential. The πN scattering amplitude at order Q^4 depends on certain combinations of low-energy constants (LECs) c_i, $\bar{d}_i$, and $\bar{e}_i$, see Refs. [15,24] for notations, which can be determined from πN scattering. Notice that at N^{3}LO, the TPEP depends on only the LECs c_i and $\bar{d}_i$. In our work [19], we employed the empirical values of the LECs c_i and $\bar{d}_i$ as found in Q^3 analyses of πN scattering. In this Letter, we adopt the values from the order Q^4 fit of Ref. [15] based on the Karlsruhe-Helsinki partial wave analysis (PWA) of πN scattering [25].

Here and in what follows, we adopt the same values for the pion and nucleon masses, pion decay constant, nucleon axial coupling constant, and pion-nucleon coupling $g_{\pi N}$ as used in Ref. [19]. We also employ the same regularization framework. In particular, the OPEP and TPEP are regularized in r space by multiplying with the function

$$f\left(\frac{r}{R}\right) = \left[1 - \exp\left(-\frac{r^2}{R^2}\right)\right]^6, \qquad (1)$$

TABLE I. χ^2/datum for the description of the Nijmegen np and pp phase shifts [23] at different orders in the chiral expansion for the cutoff $R = 0.9$ fm. Only those channels are included that have been used in the N^{3}LO/N^{4}LO fits, namely, the S, P, and D waves and the mixing angles ϵ_1 and ϵ_2.

$E_{\rm lab}$ bin	LO	NLO	N^{2}LO	N^{3}LO	N^{4}LO
Neutron-proton phase shifts					
0–100	360	31	4.5	0.7	0.3
0–200	480	63	21	0.7	0.3
Proton-proton phase shifts					
0–100	5750	102	15	0.8	0.3
0–200	9150	560	130	0.7	0.6

TABLE II. Deuteron binding energy B_d (in MeV), asymptotic S state normalization A_S (in fm$^{-1/2}$), asymptotic D/S state ratio η, radius r_d (in fm), and quadrupole moment Q (in fm^2) at various orders in the chiral expansion based on the cutoff $R = 0.9$ fm in comparison with empirical information. Also shown is the D-state probability P_D (in %). Notice that r_d and Q are calculated without taking into account meson-exchange current contributions and relativistic corrections. The star indicates an input quantity. References to experimental data can be found in Ref. [19].

	LO	NLO	N^{2}LO	N^{3}LO	N^{4}LO	Empirical
B_d	2.0235	2.1987	2.2311	2.2246*	2.2246*	2.224 575(9)
A_S	0.8333	0.8772	0.8865	0.8845	0.8844	0.8846(9)
η	0.0212	0.0256	0.0256	0.0255	0.0255	0.0256(4)
r_d	1.990	1.968	1.966	1.972	1.972	1.975 35(85)
Q	0.230	0.273	0.270	0.271	0.271	0.2859(3)
P_D	2.54	4.73	4.50	4.19	4.29	

with the cutoff R being chosen in the range of $R = 0.8$–1.2 fm. For contact interactions, we use a nonlocal Gaussian regulator in momentum space with the cutoff $\Lambda = 2R^{-1}$; see Ref. [19] for more details. We also adopt the same treatment of electromagnetic effects and relativistic corrections and employ the same fitting strategy to determine the values of the LECs accompanying contact interactions as done in Ref. [19]. In particular, we use np and pp phase shifts and mixing angles of the NPWA as input in our fits and define their errors by deviations to the results based on the Nijmegen I, II, and Reid93 NN potentials of Ref. [26], which can be regarded as alternative PWA. While χ^2/datum for the description of the Nijmegen phase shifts calculated using the errors Δ_X defined above does, clearly, *not* allow for statistical interpretation, see Ref. [19] for more details, it provides a useful tool to quantify the accuracy of the fits.

For all considered values of the cutoff, namely, $R = 0.8$, 0.9, 1.0, 1.1, and 1.2 fm, the resulting LECs are found to be natural and comparable in size with their N^{3}LO values given in Ref. [19]. We found that the inclusion of the fifth-order TPEP leads to a substantial improvement in the description of np and pp phase shifts (for hard cutoff choices). As an example, we show in Table I the resulting χ^2/datum for the description of the Nijmegen np and pp phase shifts using the cutoff $R = 0.9$ fm, which was found in Ref. [19] to yield most accurate results for NN observables. Notice that the additional IB N^{4}LO contact term affects only np results. Switching it off leads to χ^2/datum $= 0.5$ for the description of the np phase shifts in both energy bins. Further, the residual cutoff dependence of the phase shifts appears, as expected, to be very similar at N^{4}LO and N^{3}LO. Also, the error plots at N^{4}LO reveal a similar behavior to those at N^{3}LO shown in Fig. 5 of that work, so that the estimation of the breakdown scale of $\Lambda_b = 600$ MeV for $R = 0.8, \ldots, 1.0$ fm made in the N^{3}LO analysis of Ref. [19] remains valid at N^{4}LO.

For the deuteron properties, the N^{4}LO predictions are very close to those at N^{3}LO (except for P_D, which is not observable), see Table II, indicating a good convergence of the chiral expansion. This feature holds true for all choices of the cutoff R.

We now address the question of the theoretical uncertainty of our calculations due to the truncation of the chiral expansion. To this aim, we employ the approach proposed in Ref. [19], which is based on estimating the size of neglected higher-order contributions and does not rely on a cutoff variation. Specifically, the uncertainty $\Delta X^{\mathrm{N^4LO}}(p)$ of a N^{4}LO prediction $X^{\mathrm{N^4LO}}(p)$ for an observable $X(p)$, with p referring to the center-of-mass momentum, is estimated via

$$\begin{aligned}\Delta X^{\mathrm{N^4LO}}(p) = \max[&Q^6 \times |X^{\mathrm{LO}}(p)|,\\ &Q^4 \times |X^{\mathrm{LO}}(p) - X^{\mathrm{NLO}}(p)|,\\ &Q^3 \times |X^{\mathrm{NLO}}(p) - X^{\mathrm{N^2LO}}(p)|,\\ &Q^2 \times |X^{\mathrm{N^2LO}}(p) - X^{\mathrm{N^3LO}}(p)|,\\ &Q \times |X^{\mathrm{N^3LO}}(p) - X^{\mathrm{N^4LO}}(p)|].\end{aligned} \quad (2)$$

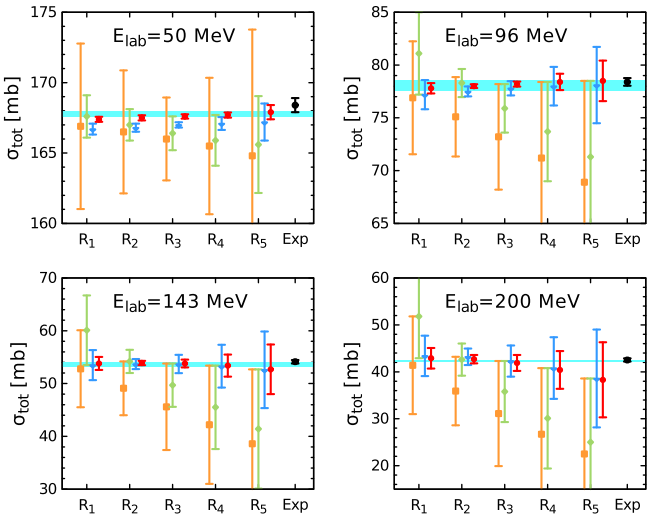

FIG. 2 (color online). Predictions for the np total cross section based on the improved chiral NN potentials at NLO (orangle filled squares), N^{2}LO (green solid diamonds), N^{3}LO (blue filled triangles), and N^{4}LO (red filled circles) for the different choices of the cutoff: $R_1 = 0.8$ fm, $R_2 = 0.9$ fm, $R_3 = 1.0$ fm, $R_4 = 1.1$ fm, and $R_5 = 1.2$ fm. The horizontal band refers to the result of the NPWA with the uncertainty estimated as explained in the text. Also shown are experimental data of Ref. [27].

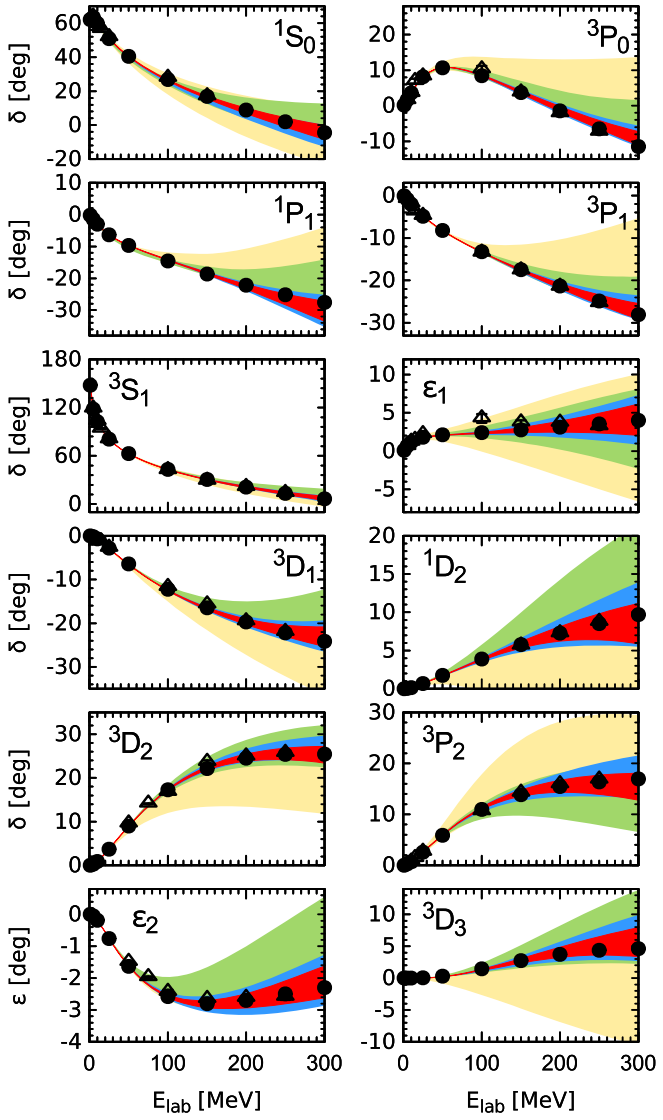

FIG. 3 (color online). Results for the np S, P, and D waves, and the mixing angles ϵ_1, ϵ_2 up to N^{4}LO based on the cutoff of $R = 0.9$ fm in comparison with the NPWA [23] (solid dots) and the single-energy PWA of [28] (open triangles). The bands of increasing width show estimated theoretical uncertainty at N^{4}LO (red), N^{3}LO (blue), N^{2}LO (green), and NLO (yellow).

Here, $Q = \max(p/\Lambda_b, M_\pi/\Lambda_b)$ is the expansion parameter. For the breakdown scale, we use the same values as in Ref. [19], namely, $\Lambda_b = 600$, 500, and 400 MeV for $R = 0.8, \ldots, 1.0$ fm, $R = 1.1$ fm, and $R = 1.2$ fm, respectively. The theoretical uncertainty at lower orders is estimated in a similar way as described in detail in Ref. [19]. Figure 2 shows the resulting predictions for the np total cross section at different energies and for all cutoff choices. First, we observe that the predictions based on different values of the cutoff R are consistent with each other with results corresponding to larger values of R being less accurate due to a larger amount of cutoff artifacts. Second, our N^{4}LO predictions provide strong support for the new approach of error estimation. In particular, the actual size of the N^{4}LO corrections is in a good agreement with the estimated uncertainty at N^{3}LO [19]. The somewhat larger N^{4}LO contributions at the lowest energy are to be expected and can be traced back to the adopted fitting strategy in the $^1S_0$ channel; see Ref. [19] for more details. Finally, our N^{4}LO results are in a very good agreement both with the NPWA and with the experimental data.

The above error analysis can be carried out for any observable of interest. Figure 3 shows the estimated uncertainty of the S-, P-, and D-wave phase shifts and the mixing angles ϵ_1 and ϵ_2 at NLO and higher orders in the chiral expansion based on $R = 0.9$ fm. The various bands result by adding or subtracting the estimated theoretical uncertainty, $\pm\Delta\delta(E_{\rm lab})$ and $\pm\Delta\epsilon(E_{\rm lab})$, to or from the calculated results. Similarly, we show in Fig. 4 our predictions for the various NN scattering observables at $E_{\rm lab} = 200$ MeV. In all cases, we observe excellent agreement with the PWA and the available experimental data, which are shown for illustrative purposes only, and confirm a good convergence of the chiral expansion. Furthermore, the N^{4}LO uncertainty bands lie within the N^{3}LO ones. This provides a strong support for reliability of the proposed approach of error estimation. Similar conclusions follow

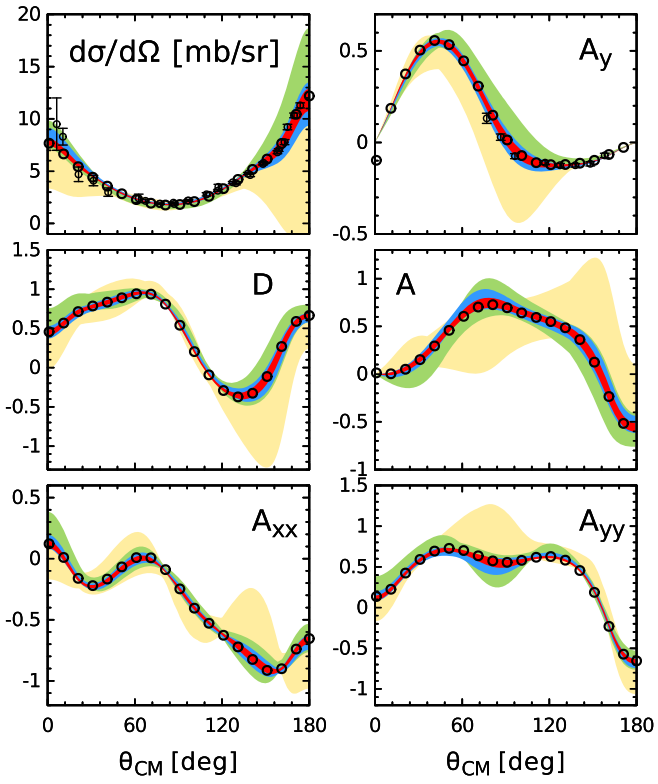

FIG. 4 (color online). Predictions for selected np scattering observables at $E_{\rm lab} = 200$ MeV calculated up to N^{4}LO based on the cutoff of $R = 0.9$ fm. Open circles refer to the result of the NPWA [23]. For remaining notations, see Fig. 3. For references to data, see [19]. $\theta_{\rm CM}$ denotes the scattering angle in the center of mass system.

from the results based on different values of the cutoff R, which are, however, less stringent due to lower accuracy of such calculations.

This work was supported by the EU (HadronPhysics3, Grant Agreement No. 283286) under the Seventh Framework Programme of EU, the ERC project 259218 NUCLEAREFT, and the DFG and NSFC (CRC 110).

[1] S. Weinberg, Phys. Lett. B **251**, 288 (1990).
[2] E. Epelbaum, H. W. Hammer, and U.-G. Meißner, Rev. Mod. Phys. **81**, 1773 (2009).
[3] R. Machleidt and D. R. Entem, Phys. Rep. **503**, 1 (2011).
[4] D. R. Entem and R. Machleidt, Phys. Rev. C **68**, 041001 (2003).
[5] E. Epelbaum, W. Glöckle, and U.-G. Meißner, Nucl. Phys. **A747**, 362 (2005).
[6] H. W. Hammer, A. Nogga, and A. Schwenk, Rev. Mod. Phys. **85**, 197 (2013).
[7] N. Kalantar-Nayestanaki, E. Epelbaum, J. G. Messchendorp, and A. Nogga, Rep. Prog. Phys. **75**, 016301 (2012).
[8] M. Viviani, L. Girlanda, A. Kievsky, and L. E. Marcucci, Phys. Rev. Lett. **111**, 172302 (2013).
[9] F. Wienholtz *et al.*, Nature (London) **498**, 346 (2013).
[10] E. Epelbaum, H. Krebs, D. Lee, and U.-G. Meißner, Phys. Rev. Lett. **104**, 142501 (2010).
[11] E. Epelbaum, H. Krebs, D. Lee, and U.-G. Meißner, Phys. Rev. Lett. **106**, 192501 (2011).
[12] E. Epelbaum, H. Krebs, T. A. Lahde, D. Lee, and U.-G. Meißner, Phys. Rev. Lett. **109**, 252501 (2012).
[13] V. Bernard, E. Epelbaum, H. Krebs, and U.-G. Meißner, Phys. Rev. C **77**, 064004 (2008).
[14] V. Bernard, E. Epelbaum, H. Krebs, and U.-G. Meißner, Phys. Rev. C **84**, 054001 (2011).
[15] H. Krebs, A. Gasparyan, and E. Epelbaum, Phys. Rev. C **85**, 054006 (2012).
[16] H. Krebs, A. Gasparyan, and E. Epelbaum, Phys. Rev. C **87**, 054007 (2013).
[17] E. Epelbaum, A. M. Gasparyan, H. Krebs, and C. Schat, Eur. Phys. J. A **51**, 26 (2015).
[18] J. Golak *et al.*, Eur. Phys. J. A **50**, 177 (2014).
[19] E. Epelbaum, H. Krebs, and U.-G. Meißner, Eur. Phys. J. A **51**, 53 (2015).
[20] R. J. Furnstahl, D. R. Phillips, and S. Wesolowski, J. Phys. G **42**, 034028 (2015).
[21] D. R. Entem, N. Kaiser, R. Machleidt, and Y. Nosyk, Phys. Rev. C **91**, 014002 (2015).
[22] See Supplemental Material at http://link.aps.org/supplemental/10.1103/PhysRevLett.115.122301, which includes Refs. [29–32], for an explicit calculation of the dominant contribution from the three-pion exchange.
[23] V. G. J. Stoks, R. A. M. Klomp, M. C. M. Rentmeester, and J. J. de Swart, Phys. Rev. C **48**, 792 (1993).
[24] N. Fettes, U.-G. Meißner, M. Mojžiš, and S. Steininger, Ann. Phys. (N.Y.) **283**, 273 (2000).
[25] R. Koch, Nucl. Phys. **A448**, 707 (1986).
[26] V. G. J. Stoks, R. A. M. Klomp, C. P. F. Terheggen, and J. J. de Swart, Phys. Rev. C **49**, 2950 (1994).
[27] W. P. Abfalterer, F. B. Bateman, F. S. Dietrich, R. W. Finlay, R. C. Haight, and G. L. Morgan, Phys. Rev. C **63**, 044608 (2001).
[28] R. A. Arndt, I. I. Strakovsky, and R. L. Workman, Phys. Rev. C **50**, 2731 (1994).
[29] A. Ekström, B. D. Carlsson, K. A. Wendt, C. Forssén, M. H. Jensen, R. Machleidt, and S. M. Wild, J. Phys. G **42**, 034003 (2015).
[30] N. Kaiser, Phys. Rev. C **61**, 014003 (1999).
[31] N. Kaiser, Phys. Rev. C **62**, 024001 (2000).
[32] N. Kaiser, Phys. Rev. C **63**, 044010 (2001).